Phase of the Atomic Polarization In High-order Harmonic-generation

Lewenstein, M; Salieres, P; L'Huillier, Anne

Published in:
Physical Review A (Atomic, Molecular and Optical Physics)

DOI:
10.1103/PhysRevA.52.4747

1995

Phase of the atomic polarization in high-order harmonic generation

Maciej Lewenstein,[1] Pascal Salières,[1] and Anne L'Huillier[1,2]
[1]*Service des Photons, Atomes, et Molécules, Centre d'Etudes de Saclay, 91191 Gif-sur-Yvette, France*
[2]*Department of Physics, Lund Institute of Technology, S-221 00 Lund, Sweden*
(Received 22 June 1995)

A recently formulated theory of high-order harmonic generation by low-frequency laser fields [Anne L'Huillier *et al.*, Phys. Rev. A **48**, R3433 (1993)] allows us to study the phase of the induced atomic dipole moment. We show that this phase exhibits a piecewise-linear dependence on the laser intensity. This dependence can be interpreted in quasiclassical terms, and is related to the action acquired by the electron during its motion in the laser field. The value of the phase, however, is also affected by the quantum effects of tunneling, diffusion, and interference. The phase of the dipole moment considerably influences the conversion efficiency, as well as the coherence properties, of the harmonics generated in macroscopic media.

PACS number(s): 32.80.Rm, 42.65.Ky

I. INTRODUCTION

High-order harmonic generation (HG) in rare gases is one of the most rapidly developing topics in the physics of atoms interacting with intense laser pulses [1–3]. The theoretical description of HG requires the solution of the time-dependent Schrödinger equation [4] describing an atom in the laser field. A good physical understanding of HG, however, is provided by a much simpler two-step model [5,6]. According to this model, the electron first tunnels [7,8] from the atomic ground state through the barrier formed by the Coulomb potential and the laser field. Its subsequent motion can be treated classically and primarily consists in oscillations of the free charge in the laser field. The electron may return to the vicinity of the nucleus and recombine to the ground state. If it returns with a kinetic energy $E_{\rm kin}$, a photon of energy $E_{\rm kin}+I_p$, where I_p is the ionization potential, may be emitted.

We have formulated recently [9,10] a fully quantum implementation of the two-step model. Our theory is a version of the strong-field approximation [7], valid in the tunneling limit $U_p \geqslant I_p > \omega$, where $U_p = E^2/4\omega^2$ is the ponderomotive potential, i.e., the mean kinetic energy acquired by the electron in the laser field of amplitude E and frequency ω. This theory is closely related to the one developed by Becker *et al.* [11]. It recovers the quasiclassical picture of the two-step model, including, at the same time, effects of quantum tunneling, diffusion, and interference.

A detailed knowledge of the single-atom dynamics is, in general, not sufficient to interpret the experimental data. To get good agreement between theory and experiment, it is necessary to account for the effects of propagation and phase matching of the harmonics in the macroscopic medium [12]. This aspect of the theory is becoming more and more important with the rapid progress of experiments addressing questions such as angular distributions [13–15], temporal [16] and spectral [17] profiles, and the precise location of the harmonic cutoff [9].

A harmonic wave generated by an atom in the presence of the laser field is usually shifted in phase with respect to the fundamental. This phase shift is equal to the phase of the atomic dipole moment induced by a (real) electromagnetic field. Obviously, if this phase depends strongly on the laser intensity, it will be different for different atoms in the interaction volume, due to the spatial variations of the intensity. In the same way, it will be time dependent, owing to the variation of the intensity during the laser pulse. In a recent Letter [18], we have shown that the phase of the dipole moment is a piecewise-linear rapidly decreasing function of U_p with a slope equal to approximately -3.2 for low intensities (when the harmonic is in the *cutoff* of the spectrum) and equal to approximately -5.8 at high intensities (when the harmonic is in the *plateau* region). The slopes are universal and depend weakly on the harmonic order. The intensity dependence of the phase plays a dramatic role in the propagation and, in particular, in the spectral and spatial coherence properties of the generated harmonic field.

This aspect of harmonic generation has been barely tackled in the literature so far. Rae *et al.* [19] have discussed the phase of the harmonic emission as a function of the position in the spectrum (plateau or cutoff). The piecewise-linear dependence of the phase on the intensity has been noted by Macklin *et al.* [1], using the model of Ref. [11]. Finally, the influence of intensity-dependent phases on the angular distributions has been pointed out by Peatross and co-workers [13,20] and by Muffet *et al.* [21].

The aim of the present paper is to investigate in detail the behavior of the phase of the dipole moment. In Sec. II we recall the expression for the induced atomic dipole moment, as follows from our theory [9,10,22]. It can be represented as a sum of contributions from (complex) trajectories of the electron. Each contribution contains a phase factor equal to the real part of the action acquired by the electron following the respective trajectory. Only those trajectories for which the action is stationary contribute to the dipole moment in a significant manner.

In Sec. III we show that, in the quasiclassical limit, there exists one dominant trajectory for which the action is stationary. For this trajectory, the return time of the electron to the nucleus is approximately 4.08 (in units in which $\omega=1$) in the cutoff and close to the full period 2π in the plateau. The phase of the induced atomic dipole can be associated with the action of the electron along this dominant trajectory. One should stress, however, that, in the plateau, there exist more

trajectories such that the action is stationary. Particularly important is the trajectory that corresponds to a rather short return time (much less than a period). To get an accurate quasiclassical approximation of the induced dipole moment, one has to account for the contribution of these two trajectories and their quantum interference [23].

In Sec. IV we discuss some of our numerical results concerning propagation effects. Here we compare conversion efficiency and spatial profiles as a function of the relative position of the atomic jet and the laser focus for various expressions of the atomic polarization. We clearly demonstrate that in order to get accurate results, one has to account very precisely for the phase of the atomic dipole and incorporate quantum interference effects. Section V contains our conclusions.

II. INDUCED ATOMIC DIPOLE MOMENT

We consider an atom in a single-electron approximation under the influence of the laser field $\vec{E}(t)$ of arbitrary polarization (we use atomic units, but express all energies in terms of the photon energy). In the length gauge, the Schrödinger equation takes the form

$$i\frac{\partial}{\partial t}|\Psi(\vec{x},t)\rangle=[-\tfrac{1}{2}\nabla^2+V(\vec{x})-\vec{E}(t)\cdot\vec{x}]|\Psi(\vec{x},t)\rangle. \quad (1)$$

$V(\vec{x})$ is the atomic potential. Initially, the system is in the ground state $|0\rangle$. We denote by $|\vec{v}\rangle$ the eigenstates of the field-free Hamiltonian corresponding to outgoing electrons with velocity $\vec{v}$.

We skip here the details of the derivation and the discussion of the validity range of our strong-field approximation, since they are thoroughly discussed in Refs. [10,22]. Within our approach, the expression for the induced atomic dipole moment $\vec{x}(t)=\langle\Psi(t)|\vec{x}|\Psi(t)\rangle$ can be written in the form of a generalized Landau-Dyhne formula [24]. We introduce a variable that is a canonical momentum

$$\vec{p}=\vec{v}+\vec{A}(t), \quad (2)$$

$\vec{A}(t)$ denoting the potential vector, and we neglect the depletion of the atomic ground state. The expression for the dipole moment is

$$\vec{x}(t)=i\int_0^t dt'\int d^3\vec{p}\;\;\vec{d}^*(\vec{p}-\vec{A}(t))\times\exp[-iS(\vec{p},t,t')]\;\;\vec{E}(t')\cdot\vec{d}(\vec{p}-\vec{A}(t'))+\text{c.c.}, \quad (3)$$

where the *quasiclassical action* is

$$S(\vec{p},t,t')=\int_{t'}^{t}dt''\left(\frac{[\vec{p}-\vec{A}(t'')]^2}{2}+I_p\right). \quad (4)$$

$\vec{d}(\vec{v})=\langle\vec{v}|\vec{x}|0\rangle$ denotes the field-free dipole transition matrix element.

Equation (3) has a physical interpretation [24] as a sum of probability amplitudes corresponding to the following processes. The last term in the integral $\vec{E}(t')\cdot\vec{d}(\vec{p}-\vec{A}(t'))$ is the probability amplitude for an electron to make the transition to the continuum at time t' with the canonical momentum $\vec{p}$. The electronic wave function is then propagated until the time t and acquires a phase factor equal to $\exp[-iS(\vec{p},t,t')]$, where $S(\vec{p},t,t')$ is the quasiclassical action. The effects of the atomic potential are assumed to be small between t' and t, so that $S(\vec{p},t,t')$ actually describes the motion of an electron freely moving in the laser field with a constant momentum $\vec{p}$. Note, however, that $S(\vec{p},t,t')$ does incorporate some effects of the binding potential through its dependence on I_p. The electron recombines at time t with an amplitude equal to $\vec{d}^*(\vec{p}-\vec{A}(t))$, which gives the first factor entering Eq. (3).

In principle, Eq. (3) can be used to evaluate $\vec{x}(t)$. The calculation of the four-dimensional integral is, however, a rather difficult task. As shown in Ref. [10], the momentum integration can be performed using the saddle-point technique. This leads to the expression for $\vec{x}(t)$ (valid in the large t limit)

$$\vec{x}(t)=i\int_0^\infty d\tau(\pi/(i\tau/2+\epsilon))^{3/2}\;\;\vec{d}^*(\vec{p}_s-\vec{A}(t))\times\exp[-iS(\vec{p}_s,t,\tau)]\;\;\vec{E}(t-\tau)\cdot\vec{d}(\vec{p}_s-\vec{A}(t-\tau))+\text{c.c.}, \quad (5)$$

from which the Fourier components

$$\vec{x}_M=\int_0^{2\pi}dt\;\;\vec{x}(t)\exp(+iMt) \quad (6)$$

can be easily calculated. In the above formulas ϵ is a small positive number, while τ denotes the electron's return time $t-t'$. The expression (5) can be easily generalized to include the effects of depletion of the ground state [10,22], but we shall not discuss this generalization here. To proceed, we have to specify the bare (field-free) atomic dipole matrix elements. For the case of hydrogenlike atoms and for transitions from s states, the field-free dipole matrix elements can be approximated by [10,25]

$$\vec{d}(\vec{p})=i\frac{2^{7/2}\alpha^{5/4}}{\pi}\frac{\vec{p}}{(\vec{p}^{\,2}+\alpha)^3}, \quad (7)$$

with $\alpha=2I_p$. The results of our approach depend, however, rather weakly on the form of $\vec{d}(\vec{p})$. This observation (discussed in detail in Refs. [10,22]) allows us to formulate a very powerful approximate expression for the Fourier components $\vec{x}_M$, using the saddle-point method applied to all five integration variables of Eq. (6), in which $\vec{x}(t)$ is replaced by the right-hand term of Eq. (3): $\vec{p}$, t, and τ.

III. QUASICLASSICAL APPROXIMATION

Since the results do not depend much on the bare atomic dipole elements, we can set $\vec{d}(\vec{p})=\text{const}$ and, for large M values,

$$\vec{x}_M \propto \int_0^{2\pi} dt \int_0^{\infty} d\tau \int d^3\vec{p} \ \exp[-iS(\vec{p},t,\tau)+iMt]. \tag{8}$$

In order to apply the saddle-point method to the above expression, we must find the stationary points of the Legendre transformed action $S(\vec{p},t,\tau)-Mt$. These stationary points are solutions of the saddle-point equations, obtained by equating the derivatives of $S(\vec{p},t,\tau)-Mt$ with respect to $\vec{p},t,\tau$ to zero:

$$\tau\vec{p}-\int_{t-\tau}^{t} dt'\vec{A}(t')=0, \tag{9}$$

$$\frac{[\vec{p}-\vec{A}(t)]^2}{2}-\frac{[\vec{p}-\vec{A}(t-\tau)]^2}{2}=M, \tag{10}$$

$$\frac{[\vec{p}-\vec{A}(t-\tau)]^2}{2}+I_p=0. \tag{11}$$

Equation (9) expresses the fact that the relevant electron trajectories correspond to the electron returning back to the starting point after the time τ, Eq. (10) expresses energy conservation, and finally, Eq. (11) (which cannot be fulfilled in the real numbers domain) describes tunneling occurring at time $t-\tau$. As discussed in Ref. [26], the above equations have typically many complex solutions.

We now restrict ourselves to the case of a linear-polarized field $\vec{E}(t)=\sqrt{4U_p}[\cos(t),0,0]$. Equation (9) implies then that the components of the momentum perpendicular to the polarization direction vanish. It reduces to a scalar equation for the remaining component of the momentum that is parallel to the polarization direction. The dipole moment $x(t)$ and its Fourier components x_M are also parallel to the polarization direction. x_M can be written as

$$x_M \propto \sum_s [1/(i\tau_s/2+\epsilon)]^{3/2}[1/\det(t_s,\tau_s)]^{1/2} \times \exp[-iS(\vec{p}_s,t_s,\tau_s)+iMt_s], \tag{12}$$

where $\det(t,\tau)$ denotes the determinant of the 2×2 matrix formed by the second derivatives of the action with respect to t and τ, at $\vec{p}_s=(p_s(t,\tau),0,0)$, with $p_s(t,\tau)$ calculated from Eq. (9). The sum in Eq. (12) extends over the *relevant* saddle points, i.e., the saddle points that are physically acceptable and that give the most significant contributions. The remaining questions are which saddle points are relevant and how are they found.

In order to answer the above question, we consider, first, the case of $I_p \to 0$. For $M \geq 3.17U_p$, i.e., when the harmonic is beyond the plateau region (i.e., in the cutoff region), there are no real solutions of the saddle-point equations. There exists, however, a complex solution $(t_s,\tau_s,\vec{p}_s)$, which we denote by $(t_2,\tau_2,\vec{p}_2)$ for reasons that will become clear later. The complex return time τ_2 for this solution has a real part that is approximately equal to 4.08. This solution describes the most significant contribution to the sum (12) and is therefore the only relevant saddle point for this regime of parameters. This *complex* saddle-point solution becomes strictly real (i.e., the imaginary parts of t_2, τ_2, and $\vec{p}_2$ vanish) as the harmonic reaches the cutoff (i.e., as $3.17U_p$ becomes equal to M) and bifurcates then into two *real* saddle-point solutions in the plateau region. The first of them, which we denote $(t_1,\tau_1,\vec{p}_1)$, corresponds to a short return time $\tau_1 \simeq 0$, whereas the other one corresponds to a return time $\tau_2 \simeq 2\pi$. It is the second solution for $I_p \neq 0$ that can be obtained by continuous deformation of $(t_2,\tau_2,\vec{p}_2)$ when the intensity passes through the cutoff region (see below) and that is why we keep the same notation for it. In principle, one could think that the second solution would be less relevant since for large τ diffusion effects become more significant. In practice, both of these solutions are equally relevant, as we shall show below. As U_p increases and reaches further thresholds ($2.4U_p \simeq M$, $2U_p \simeq M$; see Fig. 1 of [10]), more and more real solutions of the saddle-point equations appear. These, however, correspond to really long return times and electron trajectories with multiple returns to the nucleus and their contribution is indeed negligible due to quantum diffusion effects.

The situation is more complex when $I_p \neq 0$, since there are no real solutions of the saddle-point equation even in the plateau region. However, even for quite high values of $I_p \simeq 10-20$, we can identify the two solutions corresponding to $\mathrm{Re}(\tau_1) \simeq 0$ and $\mathrm{Re}(\tau_2) \simeq 2\pi$. Both of them give comparable contributions in the plateau region, with the prevailing role of the solution τ_2 corresponding to the longer return times. This is somewhat surprising, but one should keep in mind that the value of x_M is determined, in the first place, by the imaginary part of Legendre transformed action $S(\vec{p}_s,t_s,\tau_s)-Mt_s$, which (for the physically acceptable saddle points) has to be negative and causes exponential damping of the otherwise unimodular probability amplitudes. For the trajectories with the longer return time $\mathrm{Re}(\tau)$ the tunneling occurs when the laser field is close to its maximum, i.e., the potential barrier is relatively narrow. For this reason the imaginary part of the action (induced by the *imaginary* tunneling time) is relatively small. On the other hand, for the trajectories with shorter $\mathrm{Re}(\tau)$, the tunneling occurs when the laser field is much smaller, implying a larger barrier, a larger tunneling time, and a larger imaginary part of the action. The larger diffusion effects for the saddle point with larger $\mathrm{Re}(\tau)$ are thus compensated by the smaller imaginary part of the corresponding complex action. As U_p decreases, the solution $(t_2,\tau_2,\vec{p}_2)$ is smoothly deformed. When it reaches the plateau-cutoff transition, it merges into the solution identified, in the case of $I_p=0$, with $\mathrm{Re}(\tau_2) \simeq 4.08$. The solution $(t_1,\tau_1,\vec{p}_1)$ does not merge together with $(t_2,\tau_2,\vec{p}_2)$; on the contrary, it becomes unphysical since the imaginary part of the action becomes positive.

Equation (12) shows that the phase of the induced atomic dipoles is determined by the value of the action acquired along the most relevant saddle-point trajectory. Since the action is primarily determined by the ponderomotive energy [i.e., $S(\vec{p}_s,t_s,\tau_s) \simeq U_p\tau_s+\cdots$; see Refs. [10,22]], we conclude that the phase should be approximately equal to $-4.08U_p$ if the harmonic is in the cutoff and approximately equal to $-6.28U_p$ if the harmonic is in the plateau region.

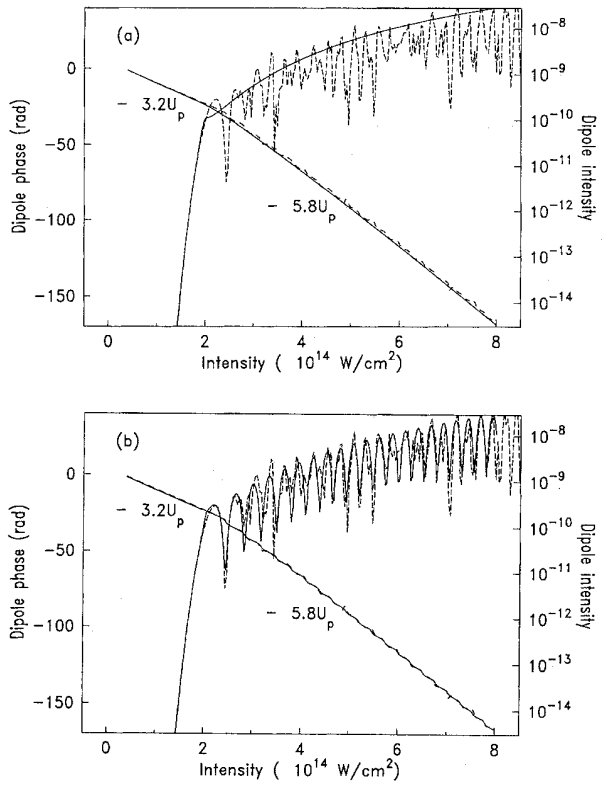

FIG. 1. Intensity and phase of the 45th harmonic emitted by a single neon atom as a function of the laser intensity. The dashed line represents the exact result and the solid line is the result of the saddle-point approximation accounting for (a) a single, most relevant, saddle point and (b) two saddle points.

Moreover, the slopes of these piecewise-linear dependences should not vary with the harmonic number or atomic species. These conclusions and rough estimates are quite accurate, as shown below, but are influenced by the complex character of the relevant electron trajectories.

In Fig. 1 we illustrate the above analysis with numerical calculations. We present the intensity dependence of the strength and phase of the 45th harmonic of 825-nm radiation, generated by a neon atom. ($I_p = 14.4$ in units of the photon energy 1.5 eV.) Dashed curves correspond to the "exact" results obtained from the solution of Eqs. (5) and (6), using hydrogenic dipole moments [Eq. (7)]. They were obtained using the technique of Bessel function expansion developed in Ref. [10]. Solid curves were obtained with the help of the saddle-point approach [Eq. (12)]. The saddle points were calculated using a two-dimensional complex Newton method. Obviously, the absolute value of the harmonic strength and phase cannot be calculated from Eq. (12) since it does not include the field-free atomic dipole matrix elements. The results obtained using the saddle-point approach were therefore normalized to the exact ones at low intensity (in the cutoff region).

In Fig. 1(a) we present the exact result (dashed curve) and the contribution of the "most relevant" saddle point, corresponding to the return time τ_2 (solid curve). The results are in excellent agreement, both for the phase and for the harmonic intensity, in the cutoff region. Note that the slope for the phase dependence ($\simeq -3.2$) is smaller than the 4.08 predicted by the rough estimate presented above. This is because the total action contains significant corrections to the ponderomotive energy contribution.

In the plateau region, the exact result is dominated by quantum interference effects. The single saddle-point approximation reproduces reasonably well the behavior of the exact curve averaged over quantum interferences, being slightly above it. In particular, the slope of the phase dependence calculated with the single saddle-point approximation, equal to -5.8 [27], coincides with the averaged slope for the exact result. We remind the reader that both the exact and the saddle-point results have been obtained neglecting depletion of the atomic ground state due to ionization. Such neglect, however, is appropriate since in the remainder of this paper we are going to consider laser pulses with the peak intensity of 6×10^{14} W/cm^2 and the effects of depletion start to play a role at intensities higher than 6×10^{14} W/cm^2.

Since propagation effects tend to wash out quantum interference effects, one could conclude from Fig. 1(a) that the single saddle-point approximation is sufficient to describe harmonic generation. In fact, a similar approximation has been used in Ref. [23] to describe the efficiency of the harmonic production as a function of laser ellipticity. However, as we show in Sec. IV, in general, such an approach is oversimplified. In particular, in order to describe the spatiotemporal coherence properties of the harmonics, it is necessary to have a better single-atom description, which can be achieved by accounting for two saddle points in the plateau region.

In Fig. 1(b) we present the same results as in Fig. 1(a), except that, for intensities at which the harmonic enters the plateau, we now account for the contribution of two saddle points, corresponding to the return times τ_1 and τ_2. As already mentioned, the saddle point $(t_1, \tau_1, \vec{p}_1)$ becomes unphysical at low intensities. We cut off its contribution in a smooth way, in order to avoid any rapid, unphysical variation of the dipole moment [28]. The agreement between the exact and the approximated result is now striking. The two saddle points account for most of the quantum interference effects in the intensity dependence of both harmonic strength and phase. One should not forget, however, that the exact result contains contributions from other electron trajectories (i.e., other relevant saddle points) and displays thus a more complex interference pattern.

The results presented here are quite general, i.e., independent of the atomic species and harmonic number. In particular, the slopes of the phase dependence on U_p are practically universal. For instance, in the cutoff, they vary from -3.15 to -3.25 between the 23rd and the 63rd harmonic in neon. In the plateau, the corresponding variation is -6.1 to -5.7. Similarly, these slopes are -3.1 and -6.1, respectively, for the 23rd harmonic in argon ($I_p = 10.5$). We conclude that the piecewise-linear behavior of the phase of the induced dipole moment is a universal property and that it can be nicely explained with the simple quasiclassical theory.

IV. ROLE OF THE PHASE IN PROPAGATION

As pointed out in Ref. [18], the phase of the induced atomic dipole moment plays a crucial role in the propaga-

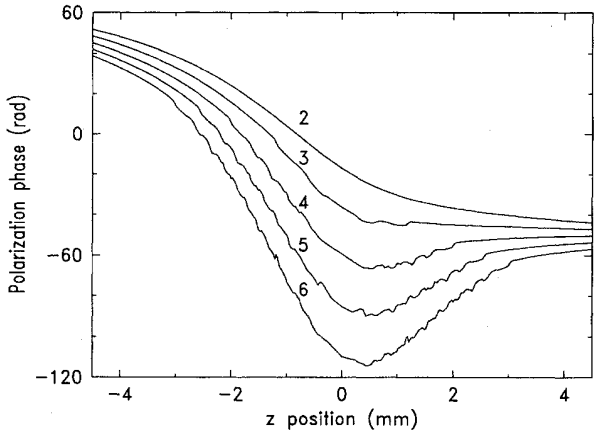

FIG. 2. Phase of the total polarization along the propagation axis (the laser is focused at $z=0$) at several laser intensities, from 2 to 6 $\times 10^{14}$ W/cm^2. The laser propagates from the left to the right.

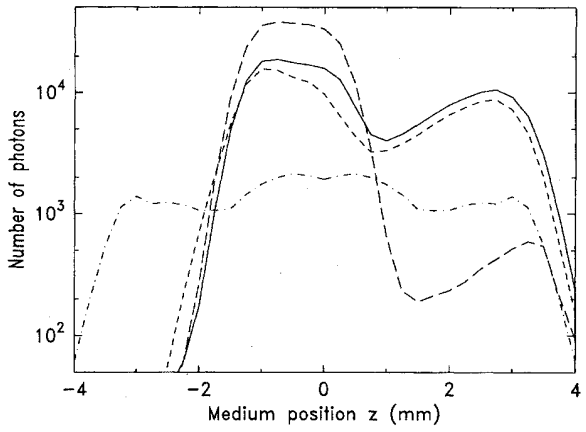

FIG. 3. Total number of photons for the 45th harmonic as a function of the position of the center of the medium z (the laser is focused at $z=0$). The dashed line represents the exact result, the long-dashed line the result of the one-saddle-point approximation, the solid line the result of the two-saddle-point approximation, and the dot-dashed line the result obtained by completely neglecting the atomic phase. The intensity of the laser pulse at the focus is 6×10^{14} W/cm^2.

tion. In Fig. 2 we show the variation of the phase of the polarization at the 45th harmonic frequency on the propagation axis z, for several peak intensities, from 2 to 6 $\times 10^{14}$ W/cm^2. Two terms contribute: (i) a propagation term induced by the phase shift of the Gaussian fundamental field, equal to $-M$ arctan$(2z/b)$ ($M=45$ and b is the confocal parameter, here equal to 5 mm), and (ii) the phase of the induced dipole moment, which depends on the z coordinate through the variation of the intensity $I(z)=I_0/(1+4z^2/b^2)$. The phase variation over the 8 mm shown in Fig. 2 is huge ($\sim$ 180 rad, i.e., 28 $\times 2\pi$) and increases with the peak intensity. The piecewise-linear intensity dependence of the atomic phase leads to a piecewise-nonlinear z dependence of the total polarization phase. The plateau-cutoff transition (which takes place at $\simeq 2.4\times 10^{14}$ W/cm^2; see Fig. 1), is observed at different $|z|$ depending on the peak intensity (e.g., at $|z|=3$ mm for $I=6\times 10^{14}$ W/cm^2). Note that the structures induced by the quantum interferences in the plateau lead to phase variations of approximately $2\pi/3$ over a very short length. As the intensity increases, the induced phase becomes more and more important in determining the total phase variation.

The phase variation is more important for negative z, where the variation of both terms, due to the induced dipole and to the propagation, add, than for positive z, where they compensate. Phase matching is optimized when the phase variation of the driving polarization is minimized over the medium length ($\simeq 1$ mm). Consequently, it strongly depends on the position of the medium relative to the laser focus. When the laser is focused *before* the generating medium (e.g., the medium is centered at $z\simeq 3$ mm for $I=6\times 10^{14}$ W/cm^2), phase matching on the optical axis is efficient and the spatial and spectral harmonics are regular and Gaussian-like [18]. When the laser is focused *in* the nonlinear medium (centered at $z=0$), the conversion efficiency is reduced due to poor phase-matching conditions, in spite of a high laser intensity in the medium. The phase fluctuations due to the quantum interference between the two most relevant electron trajectories (corresponding to τ_1 and τ_2) seem to be responsible for this effect. Finally, when the laser is focused *after* the atomic jet (e.g., centered at $z=-1$ mm for $I=6\times 10^{14}$ W/cm^2), efficient phase matching is prevented *on axis*, but becomes possible *off axis*. This leads to a high conversion efficiency, but to distorted spatial and temporal profiles (see Ref. [18]).

These points are illustrated in Figs. 3 and 4. The propagated results were obtained using the numerical methods described in Ref. [12]. The laser is supposed to be Gaussian in space and square in time. The atomic density profile is a (truncated) Lorentzian function with a 0.8 mm full width at half maximum. For the purpose of this paper, we compare the exact results with the ones obtained with the help of the quasiclassical approximation and we examine the role of the two saddle points corresponding to the return times τ_1 and τ_2. In Fig. 3 we present the conversion efficiency for the 45th harmonic as a function of the position of the center of the nonlinear medium relative to the laser focus located at $z=0$. The exact (dashed) curve exhibits clearly the two maxima corresponding to the two situations described above (phase matching on and off axis). The long-dashed line shows the result obtained with the single saddle-point approximation [see Fig. 1(a)]. It reproduces qualitatively the character of the dependence, with the two maxima. The positions of the maxima, however, are not accurate and the harmonic strength for positive values of z is evidently too small. The reason is that the maximum for positive z ($\simeq 3$ mm) occurs when the medium experiences the intensities just below (or at) the plateau-cutoff transition. In this region of intensities there are large discrepancies between the exact and single saddle-point dipoles [see Fig. 1(a)]. The exact intensity dependence of the harmonic strength has a maximum close to the plateau-cutoff transition due to the constructive interference of the two relevant electron trajectories. The single saddle-point approximation, on the other hand, does not account at all for this effect. Additionally, the latter approximation leads to a more rapid phase variation in

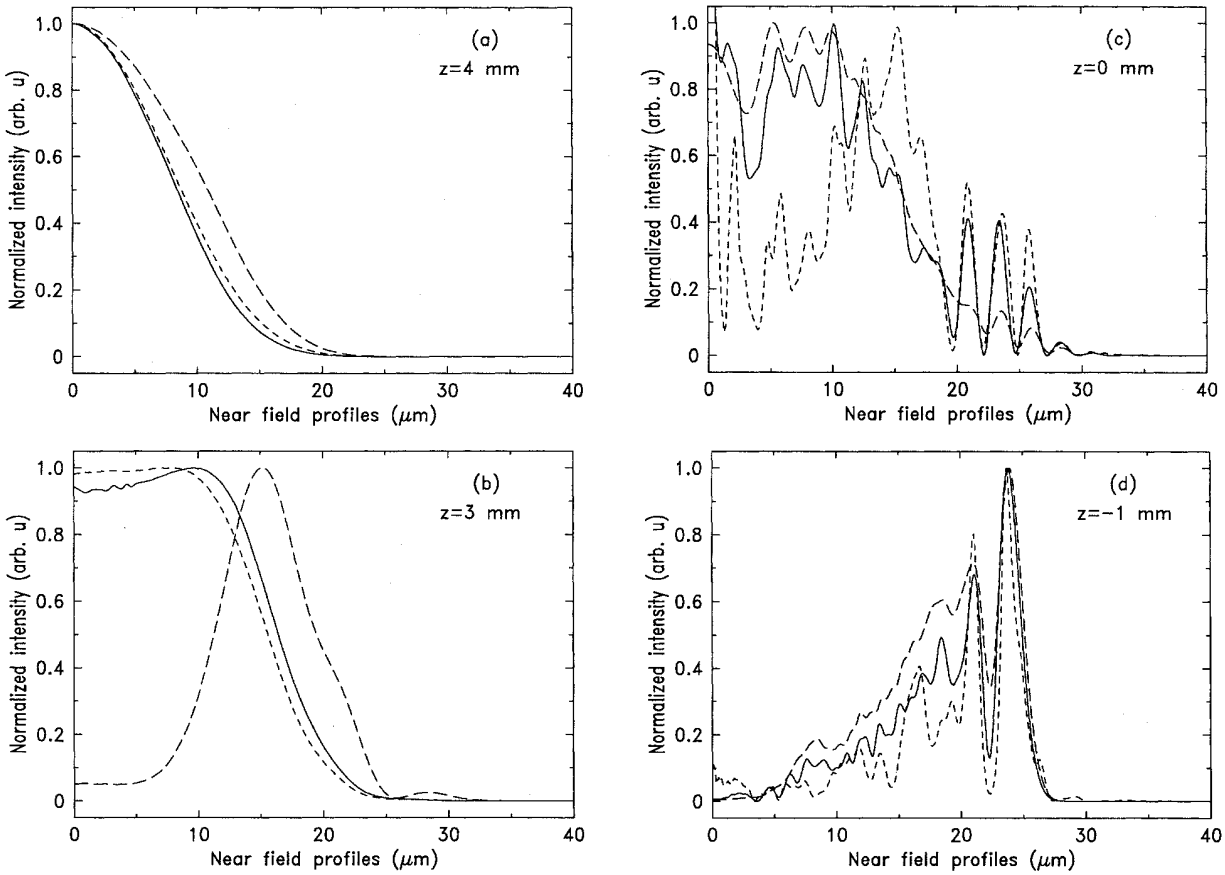

FIG. 4. Spatial profile of the 45th harmonic at the exit of the medium for a laser focus at $z=0$ and an atomic jet centered at (a) $z=4$ mm, (b) $z=3$ mm, (c) $z=0$ mm, and (d) $z=-1$ mm. The dashed line represents the exact result, the long-dashed line the result of the one-saddle-point approximation, and the solid line the result of the two-saddle-point approximation. The intensity of the laser pulse at the focus is 6×10^{14} W/cm^2.

the transition region and thus to a less efficient phase matching for positive z.

The two-saddle-point formula (solid curve) does account for the effects mentioned above and leads to propagated results that agree very well with the exact ones. For comparison, we present in Fig. 3 yet another (dot-dashed) curve, which describes the situation where the induced dipole phase is arbitrarily set to zero, keeping the exact amplitude at the dipole. In this case, efficient phase matching is practically impossible and the harmonic strength is significantly smaller than the exact one. The dependence on the jet location is flatter and, as expected, symmetric around zero.

In Fig. 4 we present spatial profiles at the exit of the nonlinear medium, for the exact (dashed curve), one-saddle-point (long-dashed curve), and two-saddle-point (solid curve) results. Figure 4(a) corresponds to $z=4$ mm. Here all the results agree and display very nice, spatially coherent Gaussian profiles. Note that the conversion efficiency, however, is quite low. For $z=3$ mm [Fig. 4(b)], i.e., at the position of one of the maxima in Fig. 3, the exact and the two-saddle-point results agree very well and give super Gaussian profiles. The one-saddle-point result, on the other hand, exhibits a different, annular, distribution. A similar situation takes place for $z=0$ mm [Fig. 4(c)], although here the differences between the exact result and two-saddle-point results are more significant. The exact curve exhibits for $z=0$ mm a clearly developed annular distribution, with erratic oscillations and an evident lack of spatial coherence. Both, the one- and the two-saddle-point results remain still more concentrated in the small divergence region. The two-saddle-point curve, however, exhibits the buildup of the same oscillatory annular structure as the exact one.

Figure 4(d) shows the results obtained when the laser is focused after the gas jet ($z=-1$ mm, corresponding to the position of the second maximum in Fig. 3). The exact and the two-saddle-point curves agree very well, giving very narrow annular distributions with overimposed oscillations. The one-saddle-point result exhibits also an annular distribution, but with a slightly smaller mean divergence and a broader annulus. These calculations point out the importance of quantum interference effects, as soon as one reaches the plateau-cutoff transition. These effects must be included in any realistic description of harmonic generation.

V. CONCLUSIONS

The phase of the induced atomic dipole moment exhibits a universal piecewise-quasilinear dependence on the laser intensity. We have given a quasiclassical interpretation of the slopes of this universal dependence in terms of the action of the most relevant electron trajectories contributing to the

harmonic-generation process in question.

The single-atom results obtained with our theoretical approach [10] can be reproduced with a simplified quasiclassical method. In this theory, the Fourier components of the induced atomic dipole are given as sums of contributions of the relevant electron trajectories. The trajectories are complex since they account for tunneling effects. For intensities corresponding to the cutoff region, there is only one relevant trajectory (corresponding to the electron returning after the time $\simeq 4$, with the maximum kinetic energy). For intensities within the plateau region, an accurate description requires to account for the contribution of two relevant trajectories, corresponding to short ($\simeq 0$) and longer return times ($\simeq 6$). The quasiclassical approximation is very accurate provided it accounts for these two trajectories. This is especially important for the detailed description of harmonic generation from macroscopic media.

Having gained confidence in the quasiclassical (saddle-point) method, we intend to generalize the results of this paper to other physically interesting cases. Several groups have begun to study experimentally harmonic generation by two colors [29]. Theoretical calculations of the atomic response to two-color laser fields are very tedious. Numerical solutions of the time-dependent Schrödinger equations require very long computational times [30]. Applications of our exact approach or of the model of Long *et al.* [31] require the use of multiple expansions of Bessel functions and are also numerically quite demanding. For these reasons, we think that the quasiclassical method provides a possible alternative tool that is fast enough to provide a sufficient amount of data of sufficient accuracy to run the propagation codes. This aspect is especially important for the two-color problem, since propagation effects are expected to play a crucial role.

ACKNOWLEDGMENTS

We acknowledge fruitful discussions with P. Agostini and K. C. Kulander.

[1] J. J. Macklin, J. D. Kmetec, and C. L. Gordon III, Phys. Rev. Lett. **70**, 766 (1993).

[2] A. L'Huillier and Ph. Balcou, Phys. Rev. Lett. **70**, 774 (1993).

[3] For more recent references, see A. L'Huillier *et al.*, J. Nonlin. Opt. Phys. Mater. **4** (1995), and references therein.

[4] J. L. Krause, K. J. Schafer, and K. C. Kulander, Phys. Rev. Lett. **68**, 3535 (1992).

[5] K. C. Kulander, K. J. Schafer, and J. L. Krause, in *Super-Intense Laser-Atom Physics*, Vol. 316 of *NATO Advanced Study Institute, Series B: Physics*, edited by B. Piraux, Anne L'Huillier, and K. Rzążewski (Plenum, New York, 1993), p. 95.

[6] P. B. Corkum, Phys. Rev. Lett. **71**, 1994 (1993).

[7] L. V. Keldysh, Zh. Éksp. Teor. Fiz. **47**, 1945 (1964) [Sov. Phys. JETP **20**, 1307 (1965)]; F. Faisal, J. Phys. B **6**, L312 (1973); H. R. Reiss, Phys. Rev. A **22**, 1786 (1980).

[8] M. V. Ammosov, N. B. Delone, and V. P. Kraĭnov, Zh. Éksp. Teor. Fiz. **91**, 2008 (1986) [Sov. Phys. JETP **64**, 1191 (1986)]; N. B. Delone and V. P. Kraĭnov, J. Opt. Soc. Am. B **8**, 1207 (1991); V. P. Kraĭnov and V. M. Ristić, Zh. Éksp. Teor. Fiz. **101**, 1478 (1992) [Sov. Phys. JETP **74**, 789 (1992)].

[9] A. L'Huillier, M. Lewenstein, P. Salières, Ph. Balcou, M. Yu. Ivanov, J. Larsson, and C. G. Wahlström, Phys. Rev. A **48**, R3433 (1993).

[10] M. Lewenstein, Ph. Balcou, M. Yu. Ivanov, A. L'Huillier, and P. Corkum, Phys. Rev. A **49**, 2117 (1994).

[11] W. Becker, S. Long, and J. K. McIver, Phys. Rev. A **41**, 4112 (1990); **50**, 1540 (1994).

[12] Our treatment of propagation effects is based on the method developed by A. L'Huillier, Ph. Balcou, S. Candel, K. J. Schafer, and K. C. Kulander, Phys. Rev. A **46**, 2778 (1992).

[13] J. Peatross and D. D. Meyerhofer, Phys. Rev. A **51**, R906 (1995).

[14] J. W. G. Tisch, R. A. Smith, J. E. Muffet, M. Ciarrocca, J. P. Marangos, and M. H. R. Hutchinson, Phys. Rev. A **49**, R28 (1994).

[15] P. Salières, T. Ditmire, K. S. Budil, M. D. Perry, and A. L'Huillier, J. Phys. B **27**, L217 (1994).

[16] M. E. Faldon, M. H. R. Hutchinson, J. P. Marangos, J. E. Muffet, R. A. Smith, J. W. G. Tisch, and C.-G. Wahlström, J. Opt. Soc. Am. B **9**, 2094 (1992); T. Starczewski, J. Larsson, C.-G. Wahlström, J.W. G. Tisch, R. A. Smith, J. E. Muffet, and M. H. R. Hutchinson, J. Phys. B **27**, 3291 (1994).

[17] C.-G. Wahlström, J. Larsson, A. Persson, T. Starczewski, S. Svanberg, P. Salières, Ph. Balcou, and A. L'Huillier, Phys. Rev. A **48**, 4709 (1993).

[18] P. Salières, Anne L'Huillier, and M. Lewenstein, Phys. Rev. Lett. **74**, 3776 (1995).

[19] S. C. Rae, K. Burnett, and J. Cooper, Phys. Rev. A **50**, 3438 (1994).

[20] J. Peatross, M. V. Fedorov, and K. C. Kulander, J. Opt. Soc. Am. B **12**, 863 (1995).

[21] J. E. Muffet, C.-G. Wahlström, and M. H. R. Hutchinson, J. Phys. B **27**, 5693 (1994).

[22] Ph. Antoine, Anne L'Huillier, M. Lewenstein, P. Salières, and B. Carré, Phys. Rev. A (to be published).

[23] In some cases it is sufficient to take the contribution of one trajectory only; cf. P. Dietrich, N. H. Burnett, M. Yu. Ivanov, and P. B. Corkum, Phys. Rev. A **50**, R3585 (1994). In general, however, calculation of observables that are affected by propagation effects requires taking into account the contributions of (at least) two trajectories.

[24] N. B. Delone and V. P. Kraĭnov, *Atoms in Strong Fields* (Springer-Verlag, Heidelberg, 1985); L. D. Landau, *Quantum Mechanics* (Pergamon, New York, 1964).

[25] H. A. Bethe and E. E. Salpeter, *Quantum Mechanics of One and Two Electron Atoms* (Academic, New York, 1957).

[26] M. Lewenstein, K. C. Kulander, K. J. Schafer, and P. Bucksbaum, Phys. Rev. A **51**, 1495 (1995).

[27] Strictly speaking, the slopes of the phase dependence are slowly varying functions of U_p. The derivative of the phase with respect to U_p is about -3.3 for small U_p and increases

slowly as U_p tends to the plateau-cutoff threshold. Above this threshold, this derivative very rapidly attains values of the order of -5.7 and -5.8 and then decreases very slowly toward an asymptotic value of -2π at $U_p \to \infty$.

[28] This is done by multiplying the contribution of the saddle point τ_1 by a factor that is 1 above the cutoff and becomes gradually smaller in the small range of intensities close to the plateau-cutoff transition.

[29] (a) M. D. Perry and J. K. Crane, Phys. Rev. A **48**, R4051 (1993); (b) S. Watanabe, K. Kondo, Y. Nabekawa, A. Sagisaka, and Y. Kobayashi, Phys. Rev. Lett. **73**, 2692 (1994); K. Kondo, Y. Kobayashi, A. Sagisaka, Y. Nabekawa, and S. Watanabe (unpublished); (c) H. Eichmann, A. Egbert, S. Nolte, C. Momma, B. Wellegehausen, W. Becker, S. Long, and J. K. McIver, Phys. Rev. A **51**, R3414 (1995).

[30] A. Sanpera (private communication).

[31] S. Long, W. Becker, and J. K. McIver, Phys. Rev. A (to be published); see also Ref. [29(b)].